

Table I. Pressure derivatives for the extremal cross section S of the electron Fermi surfaces in Pd and Pt. For comparison, the free-electron value $\frac{2}{3}K$ is given where K is the compressibility. All values are positive numbers. The values of S were taken from Refs. 2 and 4.

Orientation	$d(\ln S)/dp$ (in units of 10^{-4} kbar $^{-1}$)	
	Pd	Pt
100	4.0 ± 0.4	3.2 ± 0.3
111	3.9 ± 0.4	2.8 ± 0.3
$\frac{2}{3}K$	3.412^a	2.311^b

^aJ. A. Rayne, Phys. Rev. **118**, 1545 (1960).

^bR. E. Macfarlane, J. A. Rayne, and C. K. Jones, Phys. Letters **18**, 91 (1965).

tion and, therefore, the value quoted in Table I represents the dominant or central section.

The electron pressure derivatives in Table I show little variation with orientation. The electron surface is not highly anisotropic; it is located at the center of the Brillouin zone, and it occupies only about $\frac{1}{5}$ of the zone volume.^{2,4} Pressure, therefore, is not expected to change the anisotropy of this surface very much.

Average values of the pressure derivatives in Table I are greater than the corresponding compressibility values by about 16% in Pd and about 30% in Pt. Since these are compensated metals, the d -band hole surface and the electron surface are constrained to remain equal in volume. The calculated d -band density of states¹² at the Fermi level, however, is larger than that for the elec-

trons by at least a factor of 4. Because the pressure derivatives are not much greater than the compressibility values, then, the shift with pressure in the center of gravity of the d bands relative to the core levels is probably much smaller than the shift in the electron band relative to the Fermi level.

We would like to thank Dr. P. J. Tobin for his assistance and helpful discussions.

†Work supported in part by the Air Force Office of Scientific Research, U. S. Air Force, through Grant No. AFOSR 68-1505, and by the National Science Foundation.

¹S. Foner, R. Declo, and E. J. McNiff, Jr., J. Appl. Phys. **39**, 551 (1968).

²J. J. Vuillemin, Phys. Rev. **144**, 396 (1966).

³M. D. Stafleu and A. R. De Vroomen, Phys. Letters **19**, 81 (1965).

⁴L. R. Windmiller and J. B. Ketterson, Phys. Rev. Letters **20**, 324 (1968).

⁵J. B. Ketterson and L. R. Windmiller, Phys. Rev. Letters **20**, 321 (1968).

⁶L. R. Windmiller, J. B. Ketterson, and S. Hornfeldt, J. Appl. Phys. **40**, 1291 (1969).

⁷F. M. Mueller, Phys. Rev. **153**, 659 (1967).

⁸J. J. Vuillemin and M. G. Priestley, Phys. Rev. Letters **14**, 307 (1965).

⁹N. E. Alekseevskii, G. E. Karstens, and V. V. Mo-shaev, Zh. Eksperim. i Teor. Fiz. **46**, 1976 (1964) [translation: Soviet Phys.-JETP **19**, 1333 (1964)].

¹⁰I. M. Templeton, Proc. Roy. Soc. (London), Ser. A **292**, 413 (1966).

¹¹L. Onsager, Phil. Mag. **43**, 1006 (1952).

¹²O. K. Andersen and A. R. Mackintosh, Solid State Commun. **6**, 285 (1968).

ELECTROREFLECTANCE STUDY OF NiO

Jerrold L. McNatt

Advanced Materials Research and Development Laboratory,
Pratt and Whitney Aircraft, Middletown, Connecticut 06458

(Received 31 July 1969)

By using a thin NiO single-crystal sample, it has been possible to observe electroreflectance spectra between 3.0 and 5.0 eV. The results of this study and a recent photo-conductivity investigation suggest that an energy-band description which includes the $3d$ electrons is necessary for a full description of NiO interband optical properties.

The sensitivity to detail in the joint density of states made possible by modulation techniques¹ has not previously been utilized in studies of interband optical transitions in transition-metal compounds. This note reports electroreflectance spectra obtained for NiO and discusses their implications for three current models of electronic

structure for this material.

NiO is a NaCl-type antiferromagnet with a Néel temperature of 523°K. The specimens used in this study were prepared from a single crystal of $10^7 \Omega$ cm resistivity grown by the flame fusion technique.² Reduction in a hydrogen atmosphere at 700°C for about 10 min produced a thin nickel

metal coating through which Ohmic contact was made to the back of the sample.³ The front surface of the sample was polished until the thickness of the NiO single crystal region was about 50 μ in order to minimize the size of the dc potential drop across it. The specimen was insulated with epoxy.

Electroreflectance spectra were taken using the electrolyte technique.¹ Several different electrolytes proved equally effective but most data were obtained with buffered 0.1-N KOH. Removal of surface damage was accomplished by etching in H₃PO₄ or H₂SO₄ for several hours. The dc current through the electroreflectance cell was maintained below 20 μ A. The ratio $\Delta R/R$ was recorded directly by using electronic feedback to the photomultiplier power supply.

Spectra were obtained only when the *p*-type sample was negatively biased or positively biased to less than 1 V. This dependence on bias polarity and the previously mentioned independence of electrolyte are evidence that the $\Delta R/R$ signals originate in the NiO surface space-charge layer.

Figure 1 shows a typical $\Delta R/R$ recorder trace for NiO taken at room temperature with 9 V dc bias and 25 V peak-to-peak ac modulation at 500 Hz. The peak widths are greater than those encountered in higher-mobility semiconductors. This broadening is probably caused by a combination of the effects of stray fields due to impurities and defects introduced in the flame fusion technique of crystal growth, and the effects of strong electron-phonon coupling on the excited-state lifetime.

From the position of the first negative oscillation, the position of the "absorption edge" in NiO can be fixed as 3.7 ± 0.1 eV. Photoconductivity measurements show a steep rise at 3.7 eV which has been assigned to the absorption edge.⁴ Ab-

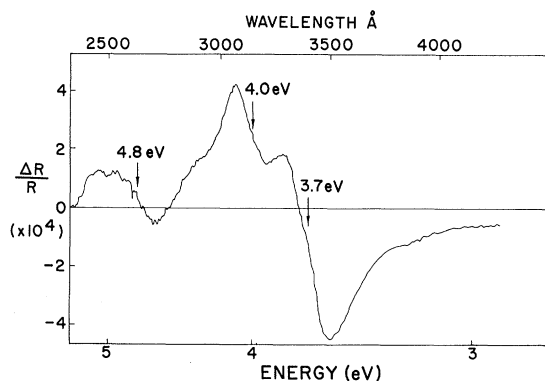


FIG. 1. Electroreflectance spectra for NiO with 9-V dc bias and 25-V peak-to-peak ac modulation.

sorption measurements can only estimate the location of this edge as approximately 4 eV because of the proximity of higher-energy crystal-field transitions and the presence of a long absorption tail below the edge which seems to be proportional to the degree of sample nonstoichiometry.⁵ (This absorption tail may be modifying the shape of the electroreflectance curves below the absorption edge.)

In Fig. 1 other oscillations are centered at 4.0 and 4.8 eV. These probably correspond to the strong reflectance peak at 4.0 eV and a small shoulder at 4.8 eV observed in recent absolute reflectivity measurements.³ Therefore, the optical and photoconductivity data impose several boundary conditions which a model of NiO electronic structure must satisfy: (1) The absorption above 3.7 eV must produce free carriers, and (2) there must be at least three critical points in the density of states between 3.7 and 4.8 eV.

Several models of NiO structure have been proposed which deal specifically with the 4-eV absorption edge. Sketches of the densities of states for these models are shown in Fig. 2, and the models are outlined below:

(a) An optical density of states for NiO has recently been derived from photoemission and reflectivity data, assuming that nondirect optical transitions dominate the spectra and that most of the structure in the ϵ_2 curves below 9 eV is due to the formation of several *p*⁵*d* localized excitons.

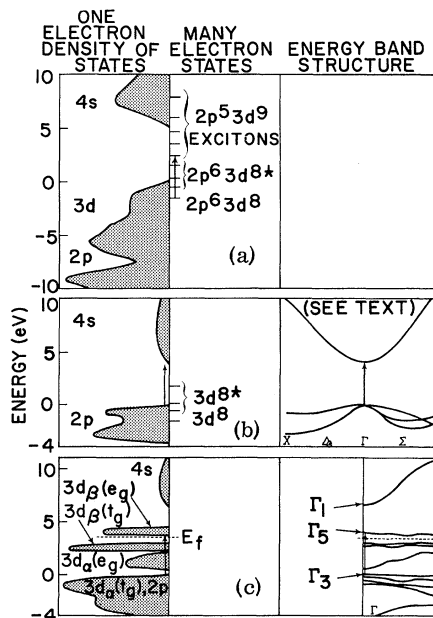


FIG. 2. Several current models for NiO absorption-edge optical structure.

The density of one-electron states, as well as the collective excitations, is shown on the left of Fig. 2(a). Transitions from $3d^8$ levels to the $4s$ conduction band begin at about 5.2 eV while the threshold for transitions from the $2p$ band to the $4s$ band appears to be near 8 eV.

(b) Another model, proposed by Feinlieb and Adler,⁶ ascribes NiO magnetic properties and crystal-field spectra (1-3.7 eV) to localized $3d$ electrons, and the electrical properties to holes in the oxygen $2p$ valence bands. The 4-eV absorption edge is assigned to transitions from the $2p$ valence bands to the nickel $4s$ conduction band. This scheme for presenting one-electron and many-electron states on a single energy-level diagram is reproduced in Fig. 2(b). The $3d$ levels are treated essentially as high-lying core electrons in this model.

(c) Augmented-plane-wave band-structure calculations have recently been undertaken by Wilson.⁷ In this model the $3d$ electrons are described as moving in narrow bands and some correlation effects are taken into account through use of a spin-polarized potential. Initial results show a gap of about 1 eV between the highest filled d band and the lowest unfilled band (also a d band). However, optical transitions between these bands are parity forbidden. The onset of strong optical absorption is predicted at 3.78 eV in the form of transitions from a narrow mixed $p-d$ band to the lowest unfilled d band. Transitions to the s band are expected at 6.5 eV. See Fig. 2(c).

The first model described above [Model (a)] proposed that the optical transitions around 4 eV are the first of a series of charge-transfer excitons. The observation of photoconductivity in high quality vapor-grown crystals⁴ in this spectral region makes this interpretation doubtful.

Model (b) fails to account for the optical structure above the absorption edge and requires an unusually small $2p-4s$ band gap. An estimate of the NiO $2p$ and $4s$ energy-band structure for Model (b) can be constructed from a nonmagnetic augmented-plane-wave energy-band calculation.⁸ This calculation shows that the $4s$ conduction band rises from a minimum at Γ to maxima at zone boundaries which lie 6 eV above the Γ minimum. The maxima of the $2p$ bands lie at Γ where all three bands are degenerate and the total bandwidth is 3 to 4 eV.⁸ In Fig. 2(b) the $4s-2p$ gap has been adjusted from the calculated value of 6.8 eV to the 4-eV value specified in Model (b). In theory, a localized set of basis states could be constructed from the $3d$ bands obtained in Ref. 8.

From these states, the localized $3d^8$ levels of Model (b) could in turn be constructed. The $4s$ and $2p$ bands predicted by Model (b) should be similar to the $3s$ and $2p$ bands of MgO since the d electrons in Model (b) are treated as core states and since both NiO and MgO have the same crystal structure and nearly identical lattice constants. Comparison of the band structure of Fig. 2(b) with a recent pseudopotential calculation⁹ for MgO shows that the shapes of the bands for the two systems are similar with the fundamental absorption edge resulting from p -to- s transitions at Γ in both cases.

In view of these considerations, only one critical point in the joint density of states for direct optical transitions should appear between the absorption edge (3.7 eV) and 5.5 eV. Three sets of electroreflectance oscillations are experimentally resolved in this range. Extra structure might occur in connection with Model (b) if the requirement of conservation of crystal momentum were relaxed due to the formation of a localized hole in the $2p$ band.¹⁰ However, the optical properties of MgO appear to be adequately described using only direct transitions.¹¹ In addition, the formation of a localized $2p$ hole in the fundamental-edge absorption process would imply that irradiation with photons of energies above 3.7 eV should produce conductivity changes dominated by the more mobile electrons in the wide $4s$ band of Model (b). A photoionization study has revealed that the holes created by photon absorption actually have drift mobilities about a factor of two greater than the electrons created by the same process.¹² This result implies that localized $2p$ holes are not formed in the 3.7-eV absorption process.

Further doubt is cast on Model (b) by comparing the suggested $2p-4s$ band gap of 4 eV with the $2p$ to $4s$ band gaps obtained in recent band-structure calculations. One calculation, which used conventional energy-band theory, obtained 6.8 eV.⁸ Another, which used a spin-polarized potential, obtained 6.5 eV.⁷ Since this gap should be relatively independent of the status of the $3d$ electrons, the $2p-4s$ band gap can be conservatively estimated to be 6.5 ± 1.0 eV, well above the 4-eV value postulated in Model (b).

Model (c) seems to fit a number of independent experimental observations. Several recent electrical measurements performed on undoped NiO yield activation energies of 1 eV between 300 and 500°K.^{11, 13-15} Model (c) explains these results as due to thermal excitation of electrons across the

1-eV gap separating the highest filled d band from the lowest unfilled d band. In addition, Model (c) assigns the optical absorption between 3.7 and 6.5 eV to transitions from $2p$ - $3d$ valence bands to an empty $3d$ band. These transitions should produce the free carriers necessary for photoconductivity, and a number of critical points will occur in the energy region of interest as Fig. 2(c) illustrates. No attempt to identify the three structures of Fig. 1 can be made until a complete band structure and density of states for NiO is available. Nevertheless, it does appear that the $3d$ electrons in NiO are formed into narrow bands and make substantial contributions to the interband density of states above the 3.7-eV absorption edge.

¹M. Cardona, K. L. Shaklee, and F. H. Pollak, *Phys. Rev.* **154**, 696 (1967).

²Samples were purchased from Marubeni-Iida, Inc., Merchandise Mart, Chicago, Ill.

³R. J. Powell, Stanford Electronics Laboratory Technical Report No. 5220-1, 1967 (unpublished).

⁴R. Newman and R. M. Chrenko, *Phys. Rev.* **114**, 1507 (1959).

⁵Ya. M. Ksendzov and I. A. Drabkin, *Fiz. Tverd.*

Tela **7**, 1884 (1965) [translation: *Soviet Phys.—Solid State* **7**, 1519 (1965)].

⁶J. Feinleib and D. Adler, *Phys. Rev. Letters* **21**, 1010 (1968), and *J. Appl. Phys.* **40**, 1586 (1969).

⁷T. M. Wilson, *J. Appl. Phys.* **40**, 1588 (1969), and Oklahoma State University, Quantum Theoretical Research Group, Research Note No. 1, 1969 (unpublished).

⁸A. C. Switendick, Massachusetts Institute of Technology, Solid State and Molecular Theory Group, Quarterly Progress Report No. 49, 1963 (unpublished).

⁹M. L. Cohen, P. J. Lin, D. M. Roessler, and W. C. Walker, *Phys. Rev.* **155**, 992 (1967); D. M. Roessler and W. C. Walker, *Phys. Rev.* **159**, 733 (1967).

¹⁰W. E. Spicer, *Phys. Rev.* **154**, 385 (1967).

¹¹I. G. Austin, A. J. Springthorpe, B. A. Smith, and C. E. Turner, *Proc. Phys. Soc. (London)* **90**, 157 (1967).

¹²V. V. Makarov, Ya. M. Ksendzov, and V. I. Kruglov, *Fiz. Tverd. Tela* **9**, 663 (1967) [translation: *Soviet Phys.—Solid State* **9**, 512 (1967)].

¹³V. P. Zhuze and A. I. Shelykh, *Fiz. Tverd. Tela* **5**, 1756 (1963) [translation: *Soviet Phys.—Solid State* **5**, 1278 (1963)].

¹⁴H. J. van Daal and A. J. Bosman, *Phys. Rev.* **158**, 736 (1967).

¹⁵M. W. Vernon and M. C. Lovell, *J. Phys. Chem. Solids* **27**, 1125 (1966).

PLANE-WAVE SOUND RADIATION FROM MOBILE DISLOCATION WALLS*

R. O. Schwenker† and A. V. Granato

Department of Physics, University of Illinois, Urbana, Illinois

(Received 29 August 1969)

Thin walls of mobile dislocations have been produced. When stimulated by a plane ultrasonic wave, the cylindrical waves radiated from each dislocation are all in phase and produce a plane radiated wave. As each dislocation contributes in the same way, the detected macroscopic plane wave directly measures the microscopic motion of individual dislocations. Radiation-induced pinning-point changes and orientation effects are evidence that the signal comes from moving and not from static dislocations.

Measurements of ultrasonic attenuation and velocity have been very useful for the study of dislocation motion and dislocation interactions with other defects, particularly with point defects and phonons.¹ Nevertheless, such studies have been indirect, requiring the interposition of a detailed theory with suitable averages to obtain quantitative results. A method for more directly obtaining information about dislocation motion is described here. This consists of putting thin walls of mobile dislocations in crystals which are subsequently driven coherently so that the walls radiate a macroscopic plane ultrasonic wave.

Lithium fluoride single crystals of dimensions

roughly $2 \times 1 \times 1$ cm, and sodium chloride crystals of dimensions roughly $2.5 \times 1 \times 1$ cm, having two sets of $\{110\}$ faces and one set of $\{001\}$ faces were used. With the long dimension of the crystal in the $[110]$ direction, a shear stress was applied on the (110) slip plane in the $[1\bar{1}0]$ slip direction. The shear deformation was introduced by mounting the specimen in a stainless steel jig, the jaws of which were polished flat to 100 ppm. The polished-jaw surfaces gripped the $(1\bar{1}0)$ faces of the crystals in order to have the stress applied on the (110) slip planes in the $[1\bar{1}0]$ slip directions. The stress to the shearing jig was supplied by a Tinius Olsen testing machine. The design of the jig was such that ultrasonic measure-